

Nearly total spin polarization in $\text{La}_{2/3}\text{Sr}_{1/3}\text{MnO}_3$ from tunneling experiments

M. Bowen, M. Bibes, A. Barthélémy, J.-P. Contour, A. Anane, Y. Lemaître, and A. Fert
*Unité Mixte de Physique CNRS / Thales, Domaine de Corbeville,
 91404 Orsay, France and Université de Paris-Sud, 91405 Orsay, France*
 (Dated: March 22, 2022)

We have performed magnetotransport measurements on $\text{La}_{2/3}\text{Sr}_{1/3}\text{MnO}_3$ / SrTiO_3 / $\text{La}_{2/3}\text{Sr}_{1/3}\text{MnO}_3$ magnetic tunnel junctions. A magnetoresistance ratio of more than 1800 % is obtained at 4K, from which we infer an electrode spin polarization of at least 95 %. This result strongly underscores the half-metallic nature of mixed-valence manganites and demonstrates its capability as a spin analyzer. The magnetoresistance extends up to temperatures of more than 270K. We argue that these improvements over most previous works may result from optimizing the patterning process for oxide heterostructures.

PACS numbers: 72.25.-b, 73.40Rw, 71.20.Eh

Magnetic tunnel junctions (MTJ) have been studied actively from the mid 90's [1] due to both the underlying physics and their potential applications as magnetic memories (MRAMs) or sensors. These structures consist of two ferromagnetic metallic electrodes (FM) sandwiching a thin insulating barrier (I). When a bias voltage V_{DC} is applied, electrons near the FM/I interface tunnel through the barrier and, since they are spin-polarized, the resistance depends on the relative orientation of the electrodes' magnetization. The tunneling magnetoresistance (TMR) ratio is defined as

$$\text{TMR} = (R_{\text{AP}} - R_{\text{P}})/R_{\text{P}} \quad (1)$$

where R_{AP} and R_{P} are the resistances of the junction in the antiparallel and parallel configurations, respectively. In Julliere's model [2], the TMR ratio is related to the spin polarizations P_1 and P_2 of the two ferromagnetic electrodes as:

$$\text{TMR} = 2P_1P_2/(1 - P_1P_2) \quad (2)$$

Within this simple model, large TMR ratios result from electrodes, or from electrode-barrier interfaces [3], with large effective spin polarization values. Junctions which integrate amorphous barriers such as Al_2O_3 and transition ferromagnets, for which the spin polarization does not exceed around 50 % [1, 4], do not show TMR ratios larger than 60 %. Preliminary work has been reported[5] on obtaining large interfacial spin polarizations owing to band structure effects, but the simplest route to achieving large TMR ratios relies on the use of so-called "half-metals" with a nearly total intrinsic spin polarization.

A few compounds have been predicted to be half-metallic, such as CrO_2 [6], Fe_3O_4 [7], mixed-valence manganites [8] or some Heusler alloys [9]. In the particular case of manganites such as $\text{La}_{2/3}\text{Sr}_{1/3}\text{MnO}_3$ (LSMO) and $\text{La}_{2/3}\text{Ca}_{1/3}\text{MnO}_3$ (LCMO), there is a lot of controversy

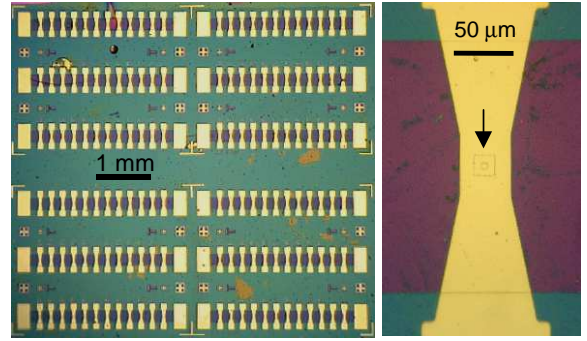


FIG. 1: Optical images of the processed sample

regarding their half-metallicity. Indeed, whereas spin-polarized photoemission spectroscopy experiments [10] have confirmed the half-metallic character of LSMO, the maximum spin polarization as inferred from tunneling experiments does not exceed 86% in LCMO [11] and 83% in LSMO [12].

In this letter, we report a TMR ratio of more than 1800 % at $T=4.2\text{K}$ and $V_{\text{DC}}=1\text{mV}$ in $\text{La}_{2/3}\text{Sr}_{1/3}\text{MnO}_3$ / SrTiO_3 / $\text{La}_{2/3}\text{Sr}_{1/3}\text{MnO}_3$ fully epitaxial MTJs, from which we deduce a spin polarization of at least 95 % for LSMO. This result confirms for the first time the transport half-metallic nature [13] of this material, which can therefore be used as a spin analyzer in tunneling experiments[3]. We argue that this large TMR value arises both from preserving the quality of the LSMO / STO (STO : SrTiO_3) interfaces during our upgraded patterning process, and from designing junctions of small size. The TMR extends to temperatures of about 280K, an improvement compared to previous results in the literature [14].

LSMO 350 Å / STO 28 Å / LSMO 100 Å epitaxial tri-layer structures were grown by pulsed laser deposition onto (001)-oriented 10 mm × 10 mm × 0.5 mm STO commercial substrates in the same conditions as in references 12 and 15. With an idea to induce a pinning effect

on the top LSMO electrode, samples were inserted into a r.f. sputtering system and 150 Å of Co were deposited, then etched by an oxygen-rich plasma to form a CoO layer some 25 Å thick. The samples were finally capped with 150 Å of gold. The LSMO in-plane cell parameters as measured by X-ray diffraction are equal to those of STO, implying that the oxide part of the heterostructure is unrelaxed from the elastic point of view[15]. Scanning electron energy loss spectroscopy (EELS) experiments performed at the atomic scale on samples grown in the same conditions revealed only a very weak modification of the electronic properties of the LSMO at the interface with the STO barrier when compared to regions located deeper inside the LSMO layer [16] (no change in the valence of the Mn ions).

The patterning process was carried out by standard UV photolithography techniques [17] using chromium masks which define 144 MTJs ranging in size from 2 to 6144 μm^2 , within a 6 mm \times 6 mm surface. In the first step, 144 pillars were defined by photolithography and ion-beam etching. During the etching process, the sample was mounted on a water-cooled sample holder. Ar ions were accelerated with a grid voltage of 200 V and neutralized by an electron-emitting filament. The etching process was monitored with an in-situ Secondary Ion Mass Spectroscopy so as to stop the etching when entering the bottom LSMO layer. In the second step, twelve 200 μm -wide bottom electrodes were created using the same combination of photolithography and neutralized ion-beam etching. To passivate the sample, a 2500 Å-thick layer of Si_3N_4 was deposited by dc-sputtering and selectively removed by reactive ion etching to define electrical access points. Finally, Ti/Au tracks were deposited as electrical contacts for transport measurements. Optical images of the completed sample are shown in Figure 1. After completing the patterning process, MTJ resistance was checked at room temperature, which revealed that the junctions of area larger than 32 μm^2 were short-circuited. Among the remaining ones, 12 could be measured.

Transport measurements were carried out in a four-point measurement configuration. The resistance of the bottom LSMO electrode was always at least one order of magnitude smaller than that of the junction so that an artificial TMR enhancement due to non-homogeneous current injection may be discounted. The LSMO bottom electrode resistivity was in the 100-120 $\mu\Omega$ cm range at $T=4\text{K}$, i.e. only about twice that of high-quality epitaxial films and single crystals and a seven-fold reduction compared to our previous process. We attribute this improvement in LSMO electrode quality to switching to a neutralized ion beam to etch the oxide layers and to cooling the sample during the etching process [18]. Given that LSMO thin films are prone to desorbing oxygen with rising temperature [19], limiting all sources of sample heating should reduce structural (and therefore magnetic and electronic) modifications of the LSMO electrodes and any possible interfacial oxygen diffusion

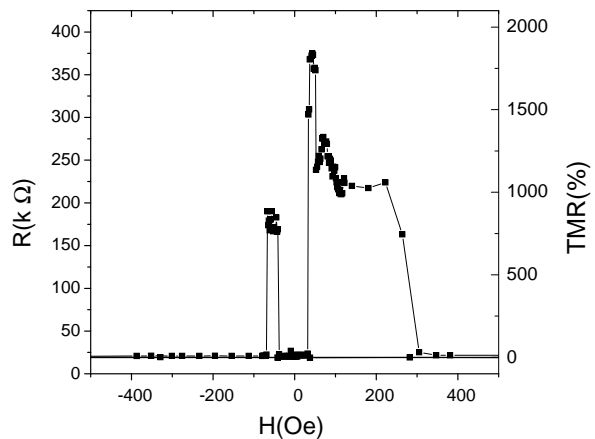


FIG. 2: $R(H)$ loop for a $5.6 \mu\text{m} \times 5.6 \mu\text{m}$ junction measured at 4.2K.

between LSMO and STO.

In Figure 2 we show the magnetic field dependence of the resistance for a $5.6 \mu\text{m} \times 5.6 \mu\text{m}$ junction, measured at 4.2K after field-cooling and with a DC bias voltage $V_{\text{DC}}=1$ mV. We recall that a Co/CoO coverage overlayer has been introduced to pin the top LSMO layer, so that, after field-cooling, a symmetric variation is not expected. When sweeping the field from negative to positive values, the resistance of the junction rises from 19 k Ω to 375 k Ω , yielding a TMR ratio of 1850 % with a field sensitivity approaching 700 %/Oe. From equation 2 and taking $P=P_1=P_2$, this value leads to a spin polarization of $P \simeq 95$ %. Four of our junctions showed a TMR larger than 800 % at 4K and 1 mV, i.e. $P > 89$ %. In addition, when increasing applied bias, the TMR decreases more rapidly than in standard MTJs with transition metal electrodes, which may be due to stronger magnon scattering [20, 21]. This suggests that a higher TMR ratio could be obtained if it were possible to measure the junction at lower applied bias.

The asymmetry in the field dependence of the TMR for this junction can be due to the shift of the magnetization reversal of the pinned layer. Upon increasing the magnetic field this separates the reversal fields of the two electrodes and leads to a well-defined and high TMR peak. In decreasing field, the two reversal fields are in the same range and the TMR is reduced. This emphasizes the need for a uniaxial anisotropy to stabilize well-defined antiparallel states like in the $\text{La}_{2/3}\text{Ca}_{1/3}\text{MnO}_3$ / NdGaO_3 / $\text{La}_{2/3}\text{Ca}_{1/3}\text{MnO}_3$ system studied by Jo *et al* [11].

The temperature dependence of the TMR is plotted in Figure 3(a, b) for two junctions using $R(H)$ loops measured at $V_{\text{DC}}=10$ mV. The TMR decreases rather quickly upon increasing T but only vanishes at temperatures of some 280K for the $2 \times 6 \mu\text{m}^2$ junction. TMR ratios of 30 % (Figure 3(c)) and 12 % are obtained at 250K and 270K, respectively. This represents a sizeable improvement with respect to previous results [12] obtained from

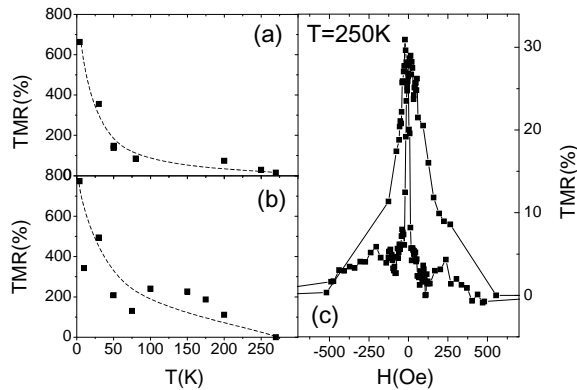


FIG. 3: Temperature dependence of the TMR measured with $V_{\text{DC}}=10$ mV for two junctions : $2 \times 6 \mu\text{m}^2$ (a) and a $1.4 \times 4.2 \mu\text{m}^2$ (b) (dashed lines are guides to the eye). $R(H)$ loop at $T=250\text{K}$ and $V_{\text{DC}}=10\text{mV}$ showing 30% TMR (c).

heterostructures grown in identical conditions. Since this system shows a temperature dependent competition between the junction dipolar field, the shape anisotropy and the CoO pinning effects described previously, it is difficult to stabilize a fully antiparallel alignment when temperature increases. This leads to a sharp extrinsic decrease of the TMR with temperature. Finally, since these results were obtained in LSMO/STO/LSMO junctions with a fully strained crystallographic structure, we state that strain is not a limiting factor toward conceiving manganite-based MTJs with sizeable TMR values at relatively high temperatures, contrary to what was sug-

gested by Jo *et al* [11]. High quality interfaces which limit the disruption of the manganite's properties fulfill a more important requisite, as suggested by previous studies [22].

In summary, we have observed a magnetoresistance of 1850 % in LSMO-based tunnel junctions, from which we deduce an average spin polarization of at least 95 % for LSMO at the interface with STO. This value may be higher at lower temperature and junction bias. As such, this result - the highest spin polarization measured in any material from tunneling experiments - underscores the transport half-metallic nature of mixed-valence manganites. In addition, the temperature dependence of the magnetoresistance for these junctions is better than previously reported, as the TMR vanishes only at about 280K. We attribute these improved results mainly to the use of an upgraded lithographic process which defines micron-sized tunnel junctions and strongly limits sample heating. Our findings show that strained LSMO can indeed be used as a spin analyzer to perform fundamental tunneling studies, possibly up to room temperature, as well as a source of fully spin polarized current in epitaxial oxide heterostructures.

Acknowledgments

We are deeply indebted to Eric Jacquet and Annie Vaures for sample growth, and to Josette Humbert for some sample processing. We acknowledge financial support within the European Union AMORE project.

-
- [1] J. Moodera, L. Kinder, T. Wong, and R. Meservey, *Phys. Rev. Lett.* **74**, 3273 (1995).
[2] M. Jullière, *Phys. Lett.* **54A**, 225 (1975).
[3] J. M. de Teresa, A. Barthélémy, A. Fert, J.-P. Contour, F. Montaigne, and P. Seneor, *Science* **286**, 507 (1999).
[4] D. Monsma and S. Parkin, *Appl. Phys. Lett.* **77**, 720 (2000).
[5] M. Bowen, C. Martínez Boubeta, V. Cros, F. Petroff, A. Fert, J. L. Costa-Krämer, J. V. Anguita, A. Cebollada, F. Briones, J. M. de Teresa, et al., *Appl. Phys. Lett.* **79**(11), 1655 (2001).
[6] S. Lewis, P. Allen, and T. Sasaki, *Phys. Rev. B* **55**, 10253 (1997).
[7] Z. Zhang and S. Satpathi, *Phys. Rev. B* **44**, 13319 (1991).
[8] W. Pickett and D. Singh, *Phys. Rev. B* **53**, 1146 (1996).
[9] R. de Groot, F. Mueller, P. van Engen, and K. Buschow, *Phys. Rev. Lett.* **50**, 2024 (1983).
[10] J. Park, E. Vescovo, H. Kim, C. Kwon, R. Ramesh, and T. Venkatesan, *Nature (London)* **392**, 794 (1998).
[11] M. H. Jo, N. D. Mathur, N. K. Todd, and M. Blamire, *Phys. Rev. B* **61**, R14905 (2000).
[12] M. Viret, M. Drouet, J. Nassar, J. Contour, C. Fermon, and A. Fert, *Europhys. Lett.* **39**, 545 (1997).
[13] I. Mazin, *Phys. Rev. Lett.* **83**, 1427 (1999).
[14] T. Obata, T. Manako, Y. Shimakawa, and Y. Kubo, *Appl. Phys. Lett.* **74**, 290 (1999).
[15] R. Lyonnet, J.-L. Maurice, M. J. Hÿtch, D. Michel, and J.-P. Contour, *Appl. Surf. Sci.* **162-163**, 245 (2000).
[16] F. Pailloux, D. Imhoff, T. Sikora, A. Barthélémy, J. Maurice, C. Colliex, and A. Fert, *Phys. Rev. B* **66**, 014417 (2002).
[17] F. Montaigne, J. Nassar, A. Vaures, F. Nguyen Van Dau, F. Petroff, A. Schuhl, and A. Fert, *Appl. Phys. Lett.* **73**, 2829 (1998).
[18] J. Z. Sun, *Physica C* **350**, 215 (2001).
[19] K. Dörr, J. M. de Teresa, K. H. Müller, D. Eckert, T. Walter, E. Vlakhov, K. Nenkov, and L. Schultz, *J. Phys. Cond. Mat* **12**, 7099 (2000).
[20] F. Guinea, *Phys. Rev. B* **58**, 9212 (1998).
[21] M. Bowen, unpublished (2002).
[22] M. Bibes, S. Valencia, L. Balcells, B. Martínez, J. Fontcuberta, M. Wojcik, S. Nadolski, and E. Jedryka, *Phys. Rev. B* **66**, 134416 (2002).